AUTOMATIC X-RAY IMAGE CHARACTERISATION for NON-DESTRUCTIVE EVALUATION

Ying Yin, Gui Yun Tian
University of Huddersfield, Queensgate, Huddersfield, HD1 3DH, UK

ABSTRACT

In this paper, firstly we introduce an automatic welding defect inspection system for X-ray image evaluation, then, a novel image segmentation approach is proposed. In this approach, we first apply an adaptive morphological filter (AMF) with an appropriate structuring element to remove noise and most of the background image which is useless for defect identification. Secondly, edges were derived from edge detection by using the Sobel operator. Morphological processing is used to make the edge continuum and calculate the defect area. The defects segmentation method is also compared with other methods. The performance of experimental results based on the proposed approach is evaluated and has been found to be appropriate for automatic radiography Non-Destructive Evaluation (NDE).

Keywords non-destructive evaluation (NDE), adaptive morphological filter (AMF), image segmentation

1 Introduction

Non-destructive testing (NDT) and non-destructive evaluation (NDE) techniques have a wide range of applications in industries via multiple methods, including Visual [1], Radiography [2], Ultrasonic [3], Eddy current [4], Acoustic emission [5] and Infrared thermography [6]. Non-destructive radiographic methods of inspection have been widely used to evaluate the integrity of material and equipment. Digital technology has been used for radiography data acquisition, radiographic image processing, defect detection and identification. Automatic defect characterisation for radiographic images is quite important especially in welded joints. These weld defects are commonly caused by porosity, slag inclusion, crack, undercut, burn through, lack of fusion, etc. [7]. However, the conventional method for non-destructive testing and evaluation is to judge the defects manually, which is not only subjective and time-consuming but also requires experienced personnel. This means that there is great demand for an automatic X-ray weld defect inspection system as shown in Fig 1.

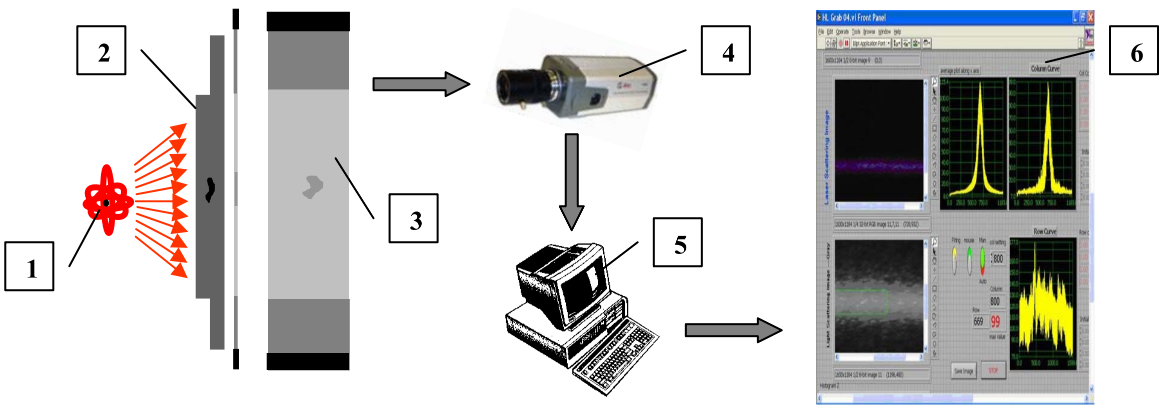

Figure 1: The automatic defect inspection system (1, the radiation source; 2, the welding specimen; 3, a piece of film; 4, a CCD camera; 5, a PC; 6, a user-friendly graphic user interface)

2 Methodologies

2.1 Automatic characterisation system for X-ray images

There are two stages for the proposed system. In stage one, the image database is designed to provide standard pictures. After applying particular image pre-processing techniques and feature extraction, the defects will be isolated from input images. The properties of defects were used for the purpose of training the artificial neural network (ANN). Furthermore, some unclassified X-ray welding images would be identified by using the trained ANN after defects segmentation step in stage two. A schematic representation of the automatic X-ray image defect evaluation system is shown in Fig 2.

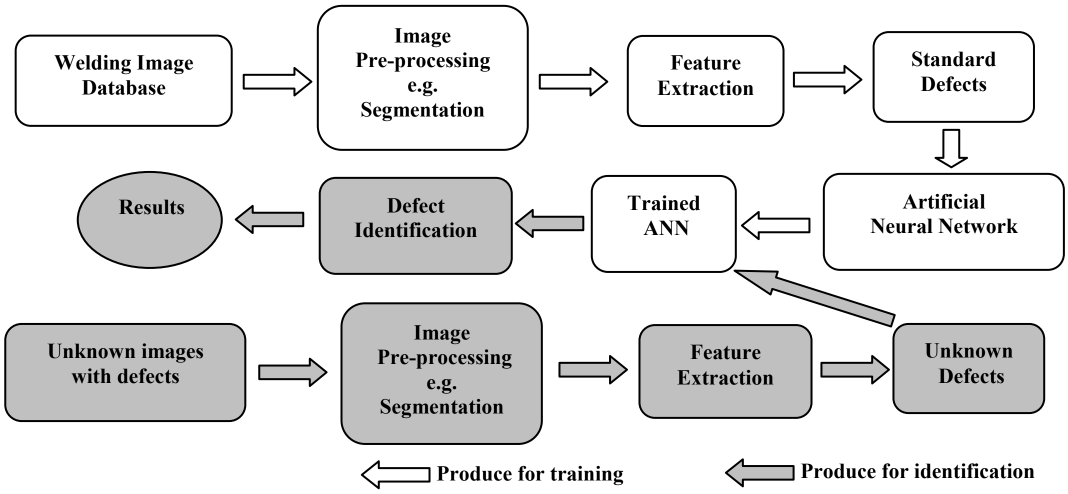

Fig 2: The main steps of the developing system

2.2 Image database

The first step in the previous flow chart is the establishment of a welding image database. The USA Standard X-ray Defect Films has been used to meet the requirements. About 183 images have been scanned at the NDT station in the Dongfang Steam Turbine Works (DFSTW), which is one of the top three turbine manufacturers in China. The USA Standard X-ray Defect Films have been used for the judgment of defects in this enterprise. It is important to train an artificial neural network (ANN) by using defects with known and typical properties (see Fig 3). After the installation (see Table 1), these images will be processed individually in order to enhance their qualities and categorised into different types of defect.

Table 1: The contents details in the image database

USA Welding Image Defects Standard (ASTM 390I)								
Varieties	Crack	LOF	LOP	BT	Porosity	SI	Undercut	Overlap
Quantities	9	11	11	4	95	45	4	4

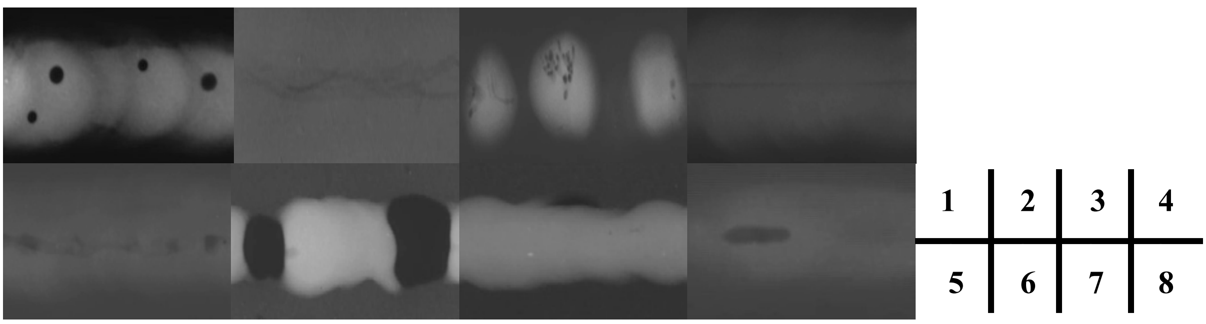

Fig 3: (1) Porosity; (2) Crack; (3) Overlap; (4) Lack of Penetration (LOP); (5) Lack of Fusion (LOF); (6) Burn Through (BT); (7) Undercut; (8) Slag Inclusion (SI)

2.3 Defects segmentation for image pre-processing

The second and also significant step in the proposed system is image pre-processing. In our specific application, the main task for image pre-processing is defect segmentation. All subsequent tasks including feature extraction and identification depend on the qualities of the image segmentation [11]. Regardless of what defect properties are taken as the judgement scale for defect identification, the defect areas should be segmented from the background image first. The most commonly used feature-domain approaches [8-10] in image segmentation include thresholding, edge detection, morphological processing, watershed transform and region growing techniques. For the proposed automatic defect inspection system, the defect segmentation can't be implemented as readily as other common applications, because of the low and various image qualities due to different scanning conditions, occurrence of multiple defects and noise in one image. It is intended to design a defect segmentation approach based on the association of adaptive morphological filters, edge detection and morphological processing. This novel and innovative image segmentation approach is outlined in the following sections.

2.3.1 Adaptive morphological filter

From the definitions of morphological operations on grey level images, it is obvious that the opening operator results in removal of narrow peaks (see Fig 4a). Closing operator (see Fig 4b) is used to remove dark details from an image which just opposite the opening operation.

(a) opening operation **(b) closing operation**

Fig 4: Examples of opening and closing operations in morphological processing

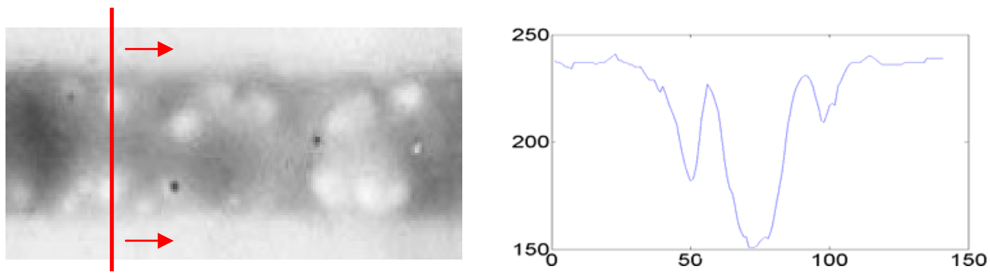

(a) the input image (grey-level) **(b) the distribution of the intensity where the red beam located**

Fig 5: The image before adaptive morphological filter

In this approach, we intend to design an adaptive morphological filter to remove noise and most of the useless background information. Firstly, a beam is used to scan the entire image row by row (see Fig 5a). There is an example to show us the distribution of the grey value where the scan beam is located in Fig 5b. The two narrow peaks in this diagram can reflect two defects areas in the input image. Based on the morphological processing theory, we implemented the opening operation on each scan beam in the input image secondly. It results in removal of the bulgy parts and keeps the cupped parts. After this process, a background image without defects can be obtained. Next image subtraction is performed as described by equations (1):

$$f_s = f - f_b \tag{1}$$

where f_s is the output image with defects only, f is the input image and f_b is the background image with noise and most other useless information.

So, the next step is how to choose the best structuring. The more appropriate structuring element we select, the better results we get. The qualities of defect shapes are dependant on the selection of structuring element. If the structuring element is not big enough, the output image might still contain some parts of the defects. However, if the structuring element is too large, it may cause the loss of background information. In this stage, we implement the watershed algorithm to each scan line; the result (see Fig 6) shows 8 different areas but only two of them are defect areas. The size of maximal area is 18. Then, an experimental test can indicate the best performance by using different structuring elements (sizes 2, 6, 10, 14, 18, 22) to do morphological processing. After the image subtraction stage, the output images have been compared as shown in Fig 7

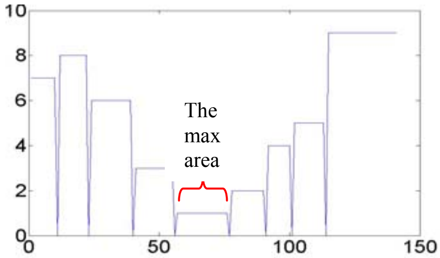

Fig 6: After watershed processing

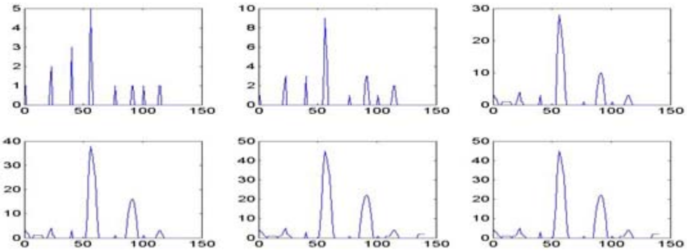

Fig 7: The comparison of different results

Based on the experimental results, the output image which uses maximal area as the structuring element and has the best performance can be easily identified. After this stage, very little background information exists and almost all the noise has been removed. Some examples using this approach are shown in Fig 8.

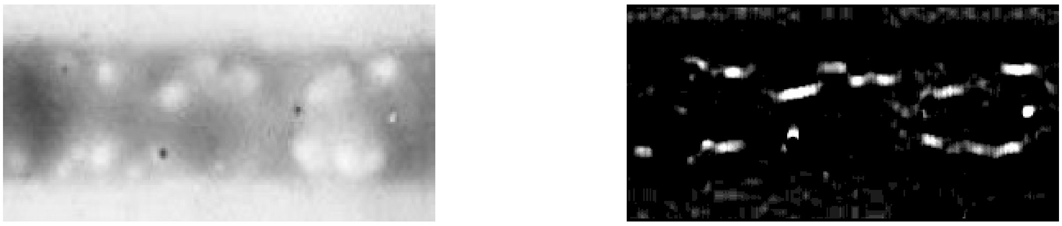

(a) the input image **(b) the output image after AMF**

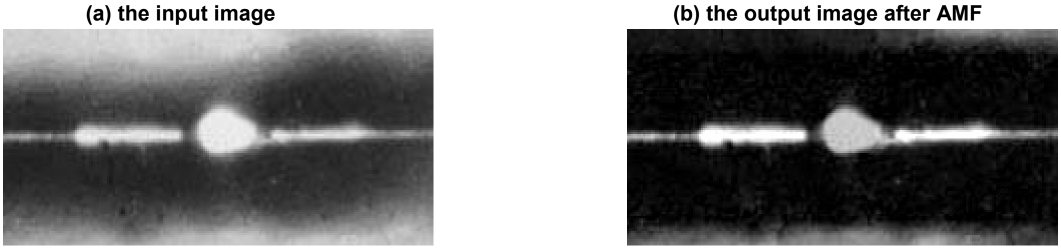

(c) the input image **(d) the output image after AMF**

Fig 8: Some examples after implemented the proposed approach.

2.3.2 Edge detection

Edges in images are places with strong contrasts jump in intensity from one pixel to the next. Edge detection in an image significantly reduces the amount of data and filters out useless information, while preserving the important structural properties in an image. The gradient method detects the edges by looking for the maximum and minimum in the first derivative of the image. The Laplacian method searches for zero crossings in the second derivative of the image to find edges [12]. The Sobel edge detector uses a pair of 3x3 convolution masks, one estimating the gradient in the x-direction and the other estimating the gradient in the y-direction. A convolution mask is usually much smaller than the actual image. As a result, the mask is slid over the image, manipulating a square of pixels at a time. The magnitude of the gradient is then calculated using the formula:

$$|G| = \sqrt{G_x{}^2 + G_y{}^2} \tag{2}$$

An approximate magnitude can be calculated using:

$$|G| = |G_x| + |G_y| \tag{3}$$

Based on the theory of Sobel edge detection, the task after the adaptive morphological filter is to transfer the grey-level image into the binary image. A comparison between two results after edge detection is shown in Fig 9. One is derived from the original image with too many artificial edges, and the other is derived from the image after AMF with the edge we wished to detect only.

Fig 9: The comparison between two result images derived from two different input images

2.3.3 Morphological processing

The two most basic morphological operators for binary images are dilation and erosion. Dilation is an operation that 'grows' or 'thickens' objects in the binary images. Mathematically speaking, dilation of *A* by *B* is denoted as $A \oplus B$, the definition is shown Eq.4:

$$A \oplus B = \{x \mid (\hat{B})_x \cap A \neq \phi\} \tag{4}$$

Where ϕ is the empty set, B is the structuring element and A is the object to be dilated. Erosion is opposite to dilation. It is an operation that 'reduces' or 'thins' objects, denoted by $A \Theta B$. The definition is shown in Eq.5

$$A \Theta B = (x \mid (B)_x \subseteq A) \tag{5}$$

Erosion is thus based on choosing the minimum value of (*f*-*b*) in a neighborhood defined by the shape of *b*. If all elements of *b* are positive, the output image is darker than the original and the effect of bright details on the input image are reduced if they cover a region smaller than *b*. The results after morphological processing can been seen in the experimental results (see Fig 11).

3 EXPERIMENTAL RESULTS

3.1 The flaw chart of the proposed approach

Based on the methodologies, we designed the image segmentation approach to follow the flow chart shown in Fig 10. At the beginning, the input image was filtered by applying AMF. The output grey level image is applied secondly as Sobel edge detection for defect isolation. After that, the morphological processing was implemented by way of edge continuum and distortion solution. Fourthly, the defect areas were outlined and the output image with defects only obtained.

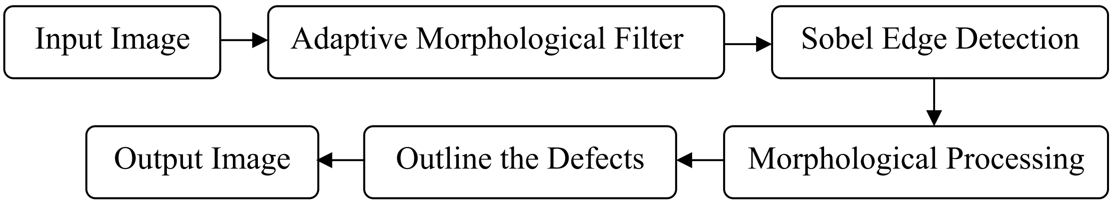

Fig 10: The flaw chart of the proposed defects segmentation approach.

3.2 Experimental results discussion

The experimental tests have been carried out under MATLAB7.0. The output images after each step were listed in Fig 11. Dilation operation results in making the edge continuum (see Fig 11a). It is obvious that in Fig 11b, the defect area after fill operation has a small amount of distortion. The following task is to isolate the real defect areas without any distortion by using erosion operation with appropriate structuring elements. After outlining the defects, we can see the shape after segmentation is quite a good match to the original defect area. This means that, the proposed image segmentation approach can provide us with brilliant results.

(a) after dilation **(b) fill the defects area** **(c) after erosion**

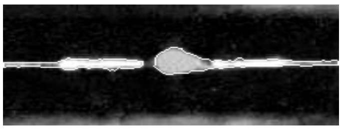

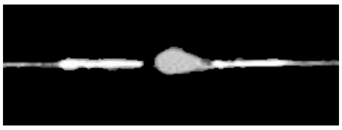

(c) after outline **(d) final result**

Fig 11: The individual images during the morphological processing

4 CONCLUSIONS and FURTHER WORK

The image database has been established to provide abundant image resources for investigation and typical defect properties for training the artificial neural network (ANN). The experimental results have proved that the adaptive morphological filter (AMF) is an effective method for noise removal and useless information reduction. The Sobel operator was selected to do the edge detection. In morphological processing, dilation is used to fill small holes and narrow gulfs in objects and erosion is used to smooth the object in order to make the segmented object look more natural. Further work will include refining the defect segmentation approach and training the ANN by using standard images after segmentation. A User-friendly graphic user interface (GUI) will be developed to enhance the manipulation and simplify the operational process for the automatic defect inspection system.

REFERENCES

1. Kyoung-Ok Kim, In-sook Jung, Sung Nam Oh, Jong-Hun Lee, Young-Kyu Yang, "Development of an image analysis system with advanced visualtechnique", Geoscience and Remote Sensing Symposium Proceedings, 1998. IGARSS apos; 98. 1998 IEEE International, Volume 2, Issue, 6-10 Jul 1998 Page(s):1079 - 1082 vol.2
2. Wernick M N, Wirjadi O, Chapman D, Oltulu O, Zhong Zhong, Yongyi Yang, "Preliminary investigation of a multiple-image radiography method", 2002 IEEE International Symposium on Biomedical Imaging, 2002, Proceedings. 7-10 July 2002 Page(s):129 - 132
3. Hung-Yang Yeh and Jung-Ho Cheng, "NDE of metal damage: ultrasonics with a damage mechanics model", International Journal of Solids and Structures, Volume 40, Issue 26, December 2003, Pages 7285-7298
4. Tian G Y, Sophian A, Taylor D, Rudlin J, "Wavelet-based PCA defect classification and quantification for pulsed eddy current NDT", Science, Measurement and Technology, IEE Proceedings-Volume 152, Issue 4, 8 July 2005 Page(s):141 – 148
5. Cherfaoui M, "Application of neural networks technique for acoustic emission NDT method", 6th European Conference on Non Destructive Testing, Nice (France), 24–28 Oct. 1994. Vol. 1, pp. 489–491. ECNDT (1994), NDT & E International, Volume 29, Issue 1, February 1996, Page 55
6. Francisco J Madruga, Daniel A González, Jesús M Mirapeix and José M López Higuera, "Application of infrared thermography to the fabrication process of nuclear fuel containers", NDT & E International, Volume 38, Issue 5, July 2005, Pages 397-401
7. Alaknanda R S Anand and Pradeep Kumar, "Flaw detection in radiographic weld images using morphological approach", NDT & E International, Volume 39, Issue 1, January 2006, Pages 29-33
8. Wang X, Wong B S, Bai W M, Tui C G, "X-ray image segmentation using wavelet method", Control, Automation, Robotics and Vision Conference, ICARCV 8th Volume 2, 6-9 Dec. 2004 Page(s):1129 - 1133 Vol. 2
9. El-Kwae E A, Tzacheva A, Kellam J F, "Model-based bone segmentation from digital X-ray images", Engineering in Medicine and Biology, 2002, Proceedings of the 24th Annual Conference and the Annual Fall Meeting of the Biomedical Engineering Society, EMBS/BMES Conference, 2002.
10. Neubauer C, Hanke R, "Electronic Improving X-ray inspection of printed circuit boards by integration of neural network classifiers", Manufacturing Technology Symposium, 1993, Fifteenth IEEE/CHMT International 4-6 Oct. 1993 Page(s):14 - 18.
11. Guojin Li, Guorong Wang, Jiquang Zhong, "A genetic algorithm on welding seam image segmentation", The Proccedings of Fifth World Congress on Intelligent Control and Automation, WCICA 2004. Vol. 3, 15-19, June 2004 2004, Page(s): 2176-2178.
12. Qiang Ji and Robert M Haralick, "Efficient facet edge detection and quantitative performance evaluation", Pattern Recognition, Volume 35, Issue 3, March 2002, Pages 689-700.